

## Supporting information:

### Understanding nitrate formation in a world with less sulfate.

1

Petros Vasilakos<sup>1</sup>, Armistead Russell<sup>2</sup>, Rodney Weber<sup>3</sup>, and Athanasios Nenes<sup>1,3,4,5†</sup>

<sup>1</sup> School of Chemical and Biomolecular Engineering, Georgia Institute of Technology, Atlanta, Georgia, 30332, USA

<sup>2</sup> School of Civil and Environmental Engineering, Georgia Institute of Technology, Atlanta, Georgia, 30332, USA

<sup>3</sup> School of Earth and Atmospheric Sciences, Georgia Institute of Technology, Atlanta, Georgia, 30332, USA

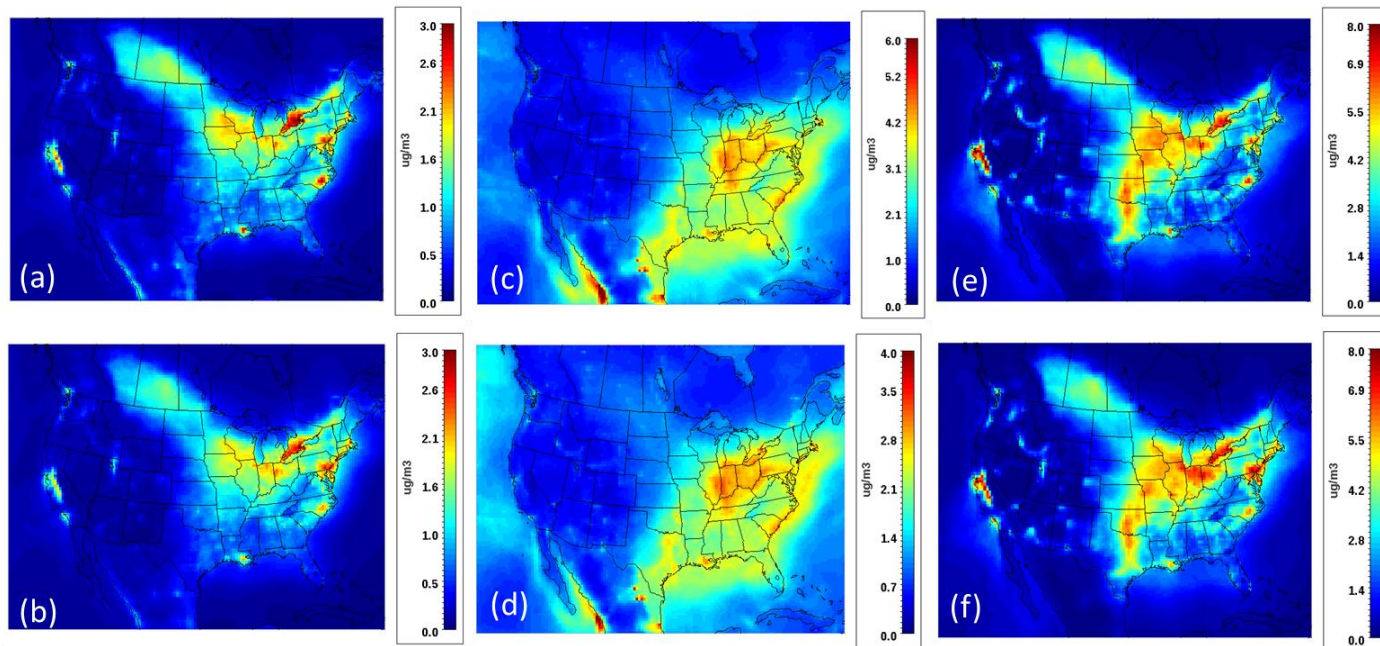
<sup>4</sup> Institute of Chemical Engineering Sciences, Foundation for Research and Technology-Hellas, Patras, GR 26504, Greece

<sup>5</sup> Institute for Environmental Research and Sustainable Development, National Observatory of Athens, Palea Penteli, GR 15236, Greece

†Corresponding Author: A. Nenes ([athanasios.nenes@gatech.edu](mailto:athanasios.nenes@gatech.edu))

2

3



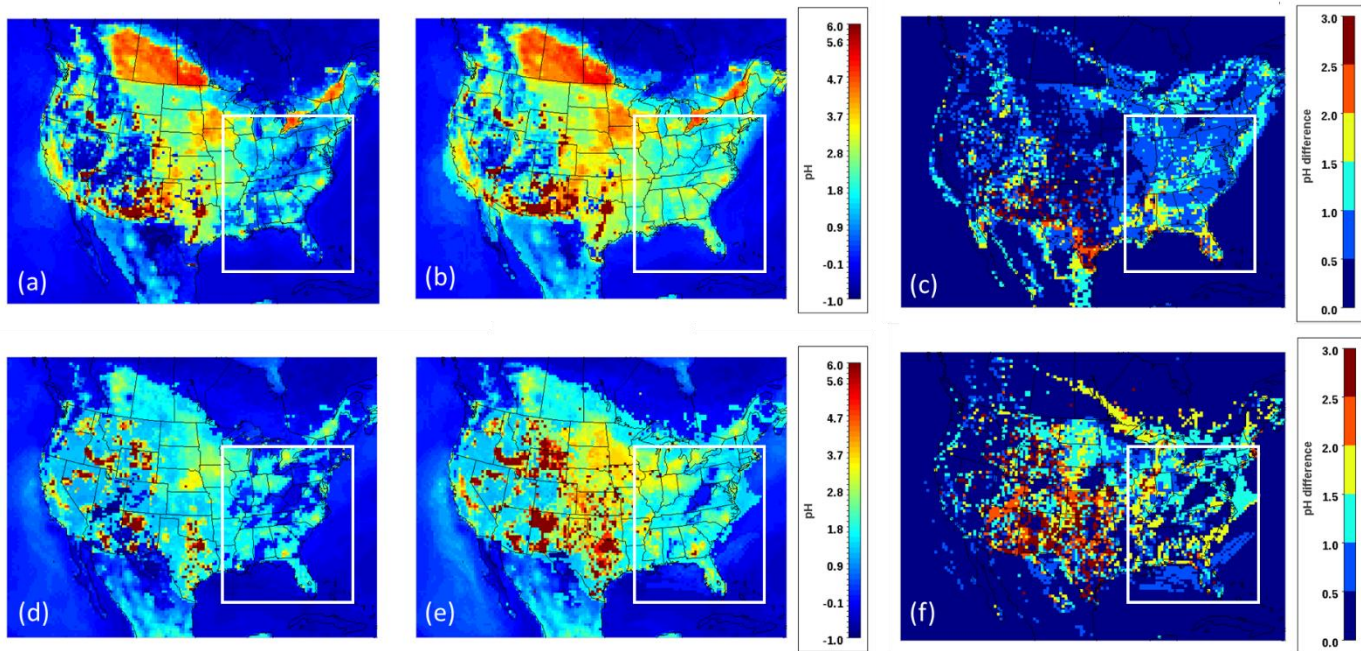
4  
 5 **Figure S1** - Yearly averaged predicted concentration fields of (a) 2001  $\text{NH}_4$ , (b) 2011  $\text{NH}_4$ , (c)  
 6 2001  $\text{SO}_4$  (d) 2011  $\text{SO}_4$ , (e) 2001  $\text{NO}_3$ , (f) 2011  $\text{NO}_3$ . Color scales between years are kept the same  
 7 for parity, except for sulfate, due to its drastic reduction during the decade

8  
 9 **Table S1** – Yearly domain averages and standard deviations for ammonium, sulfate and nitrate  
 10 in  $\mu\text{g m}^{-3}$  for 2001 & 2011

2001	$\text{NH}_4$	$\text{SO}_4$	$\text{NO}_3$	2011	$\text{NH}_4$	$\text{SO}_4$	$\text{NO}_3$
<b>Domain average</b>	0.42	1.67	1.28	<b>Domain average</b>	0.40	1.20	1.27
<b>St.dev</b>	0.47	1.02	1.43	<b>St.dev</b>	0.45	0.63	1.48

11

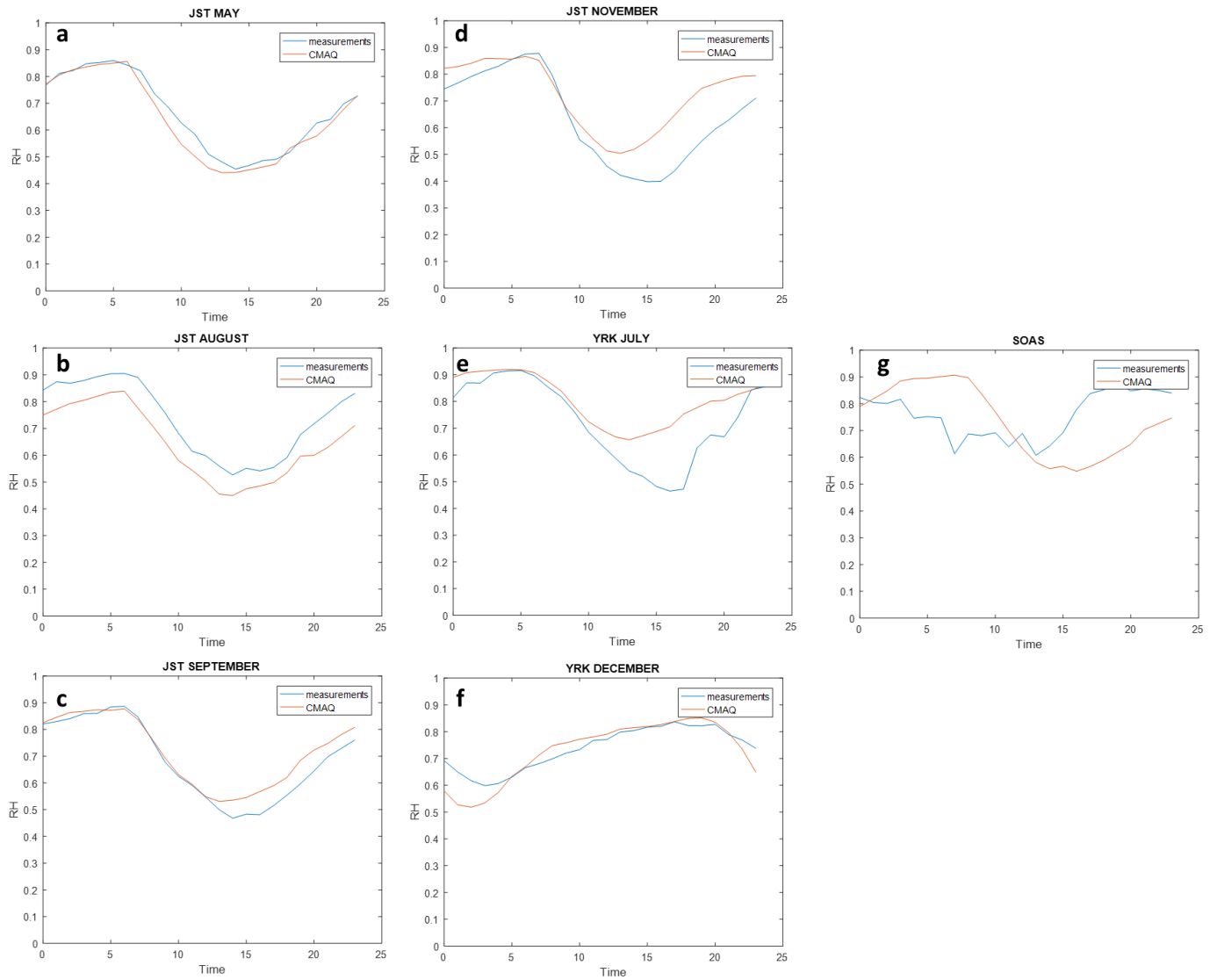
12



13

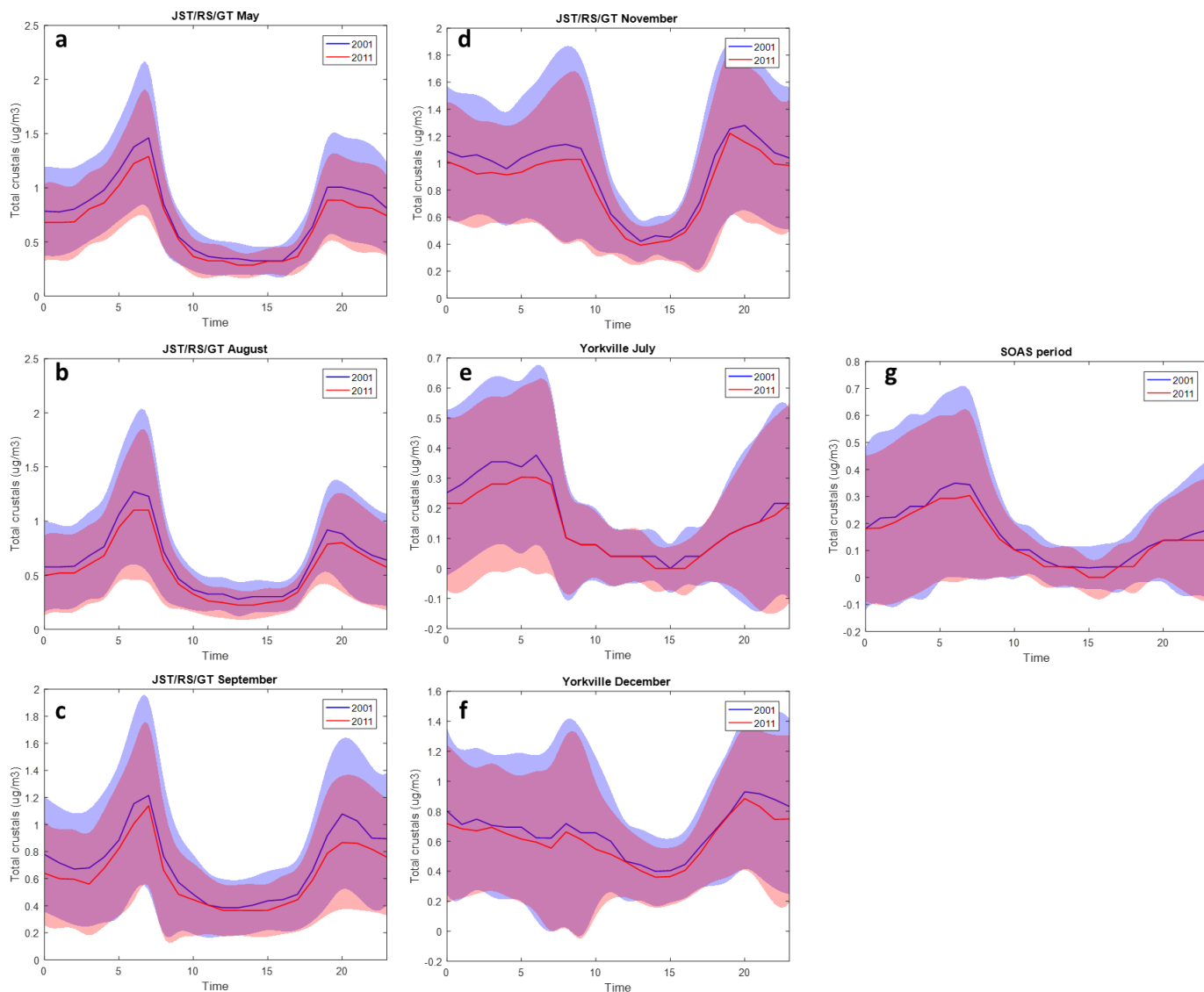
14 **Figure S2** - Seasonally averaged pH over CONUS for the winter (January) of (a) 2001, (b) 2011,  
 15 the summer (July) of (d) 2001, (e) 2011. Panel (c) is difference between the simulation years for  
 16 the winter, and (f) is the difference for the summer. As in Figure 3, the study domain is highlighted.

17



18  
 19 **Figure S3** – RH diurnal profiles for May (a), August (b), September (c) and November (d) at  
 20 JST/RS/GT, July (e) and December (f) at YRK and for the SOAS campaign period (g). Blue line  
 21 is the CMAQ predicted RH for 2001 and 2011, while the red line represents the measurements

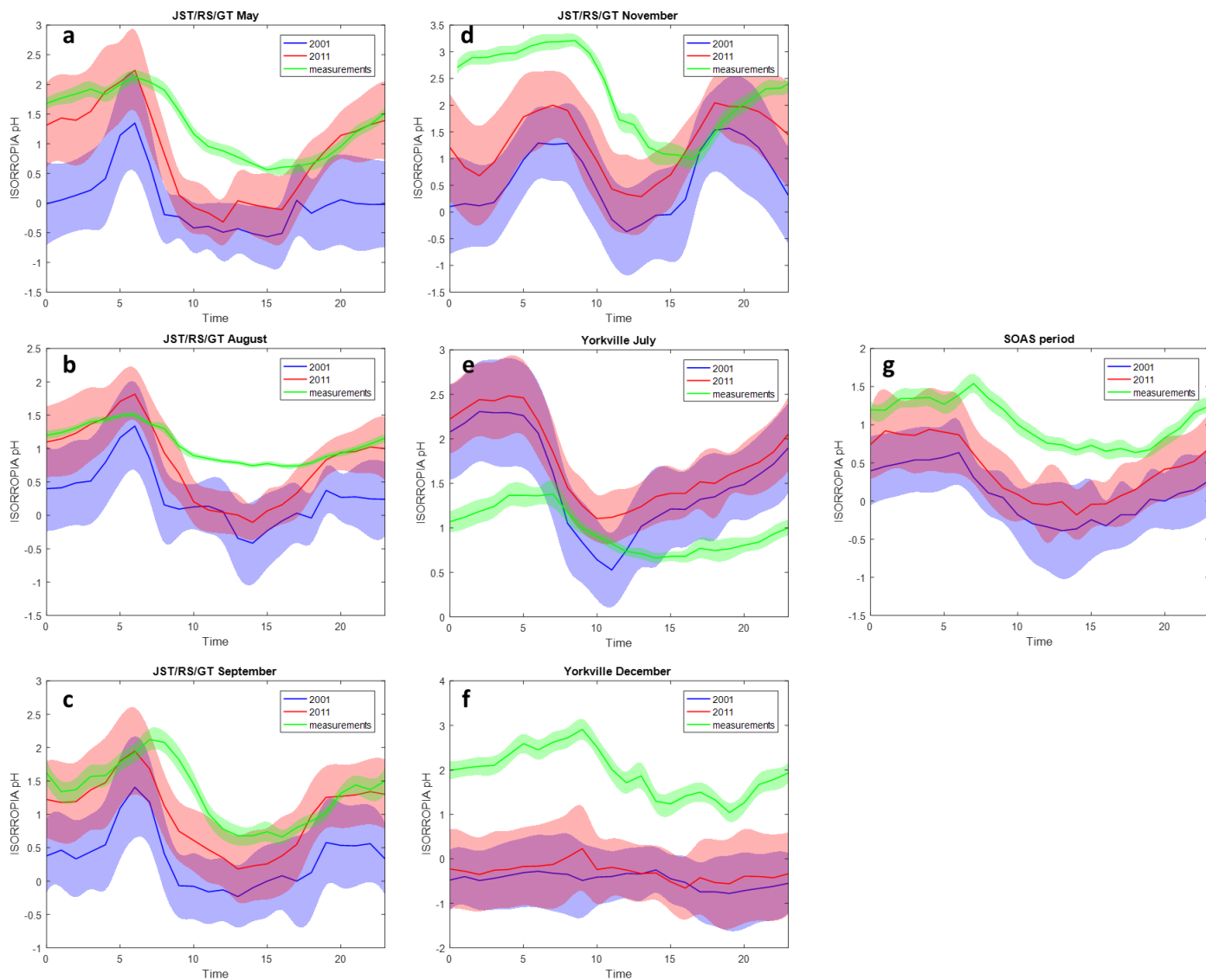
22



23

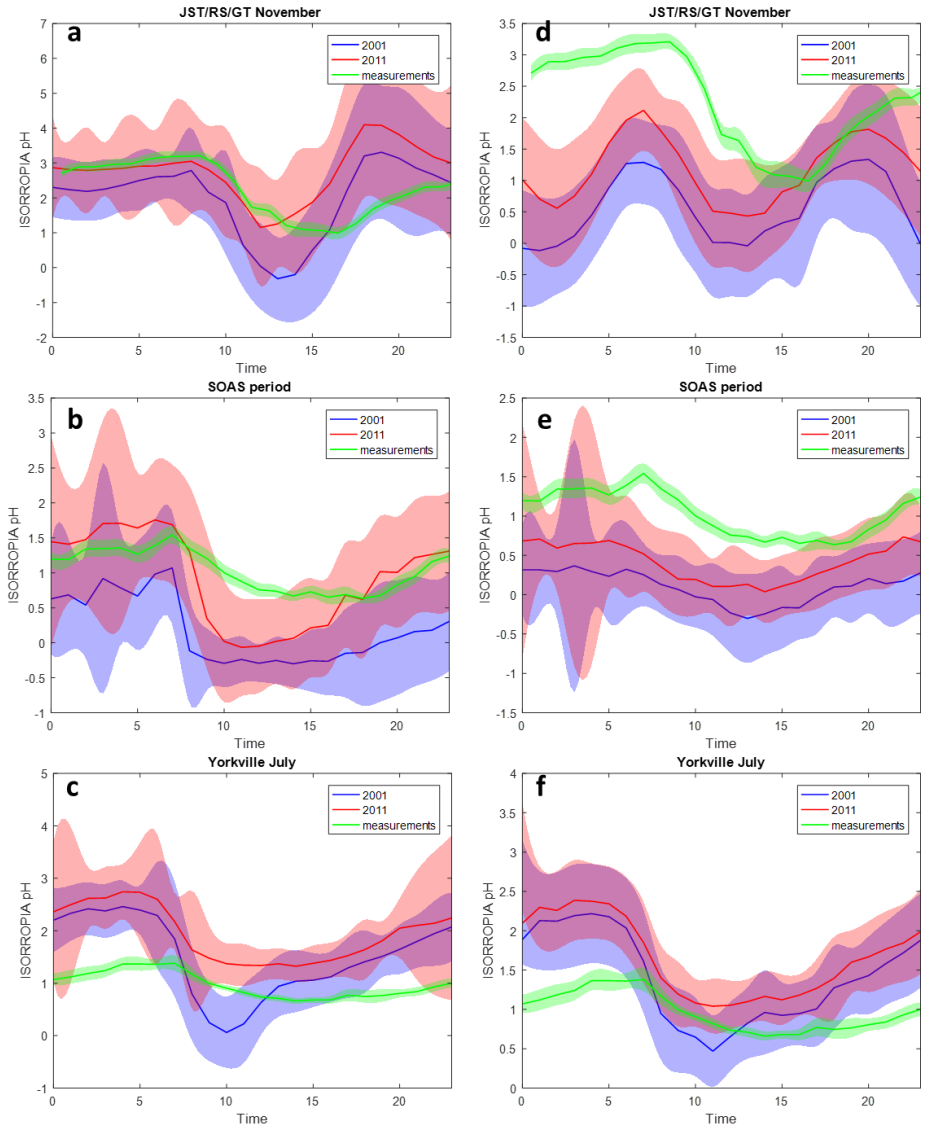
24 **Figure S4** – Total NVC diurnal profiles ( $\text{Na}^+$ ,  $\text{Ca}^{+2}$ ,  $\text{K}^+$  and  $\text{Mg}^{+2}$ ) for May (a), August (b),  
 25 September (c) and November (d) at JST/RS/GT, July (e) and December (f) at YRK and for the  
 26 SOAS campaign period (g). Blue and red lines are the CMAQ predicted NVCs for 2001 and 2011  
 27 respectively, while the shaded areas are one model standard deviation.

28



29  
 30 **Figure S5** – pH diurnal profiles when not accounting for NVCs, for May (a), August (b),  
 31 September (c) and November (d) at JST/RS/GT, July (e) and December (f) at YRK and for the  
 32 SOAS campaign period (g). Blue and red lines are the CMAQ predicted pH for 2001 and 2011  
 33 respectively, while the shaded areas are one model standard deviation. Green line represents the  
 34 measurements and the shades area is standard error.

35



36

37 **Figure S6** – pH diurnal profiles with assimilated RH when NVCs are included in the calculations,  
 38 for November at JST/RS/GT (a), the SOAS period (b) and July at YRK (c), and when NVCs are  
 39 not included for November at JST/RS/GT (d), the SOAS period (e) and July at YRK (f). Blue and  
 40 red lines are the CMAQ predicted pH for 2001 and 2011 respectively, while the shaded areas are  
 41 one model standard deviation. Green line represents the measurements and the shades area is  
 42 standard error.

43



## 44 **Organic acids and pH**

45 To determine the impact of organic compounds on acidity we tested a variety of scenarios  
46 for our CMAQ results at the SEARCH sites, using the web-version of the Extended Aerosol  
47 Inorganics Model (E-AIM) model (Wexler & Clegg 2002, Friese & Ebel 2010, Clegg et al. 1992)  
48 (<http://www.aim.env.uea.ac.uk/aim/aim.php>). More specifically, we assumed that a set amount  
49 (25 or 50% on a mole basis) of either oxalic, maleic, succinic or malonic acid already exists in the  
50 aerosol phase but is not accounted for. Given the constant reductions in sulfate, we also tested the  
51 potential of sulfate to be substituted by the same organics. To avoid the potential biases that NVCs  
52 can incur on simulations, all runs were conducted without them. E-AIM was run using the  
53 comprehensive Model IV configuration, in metastable mode. The baseline case that we used, was  
54 the average composition, temperature and RH across all sites.

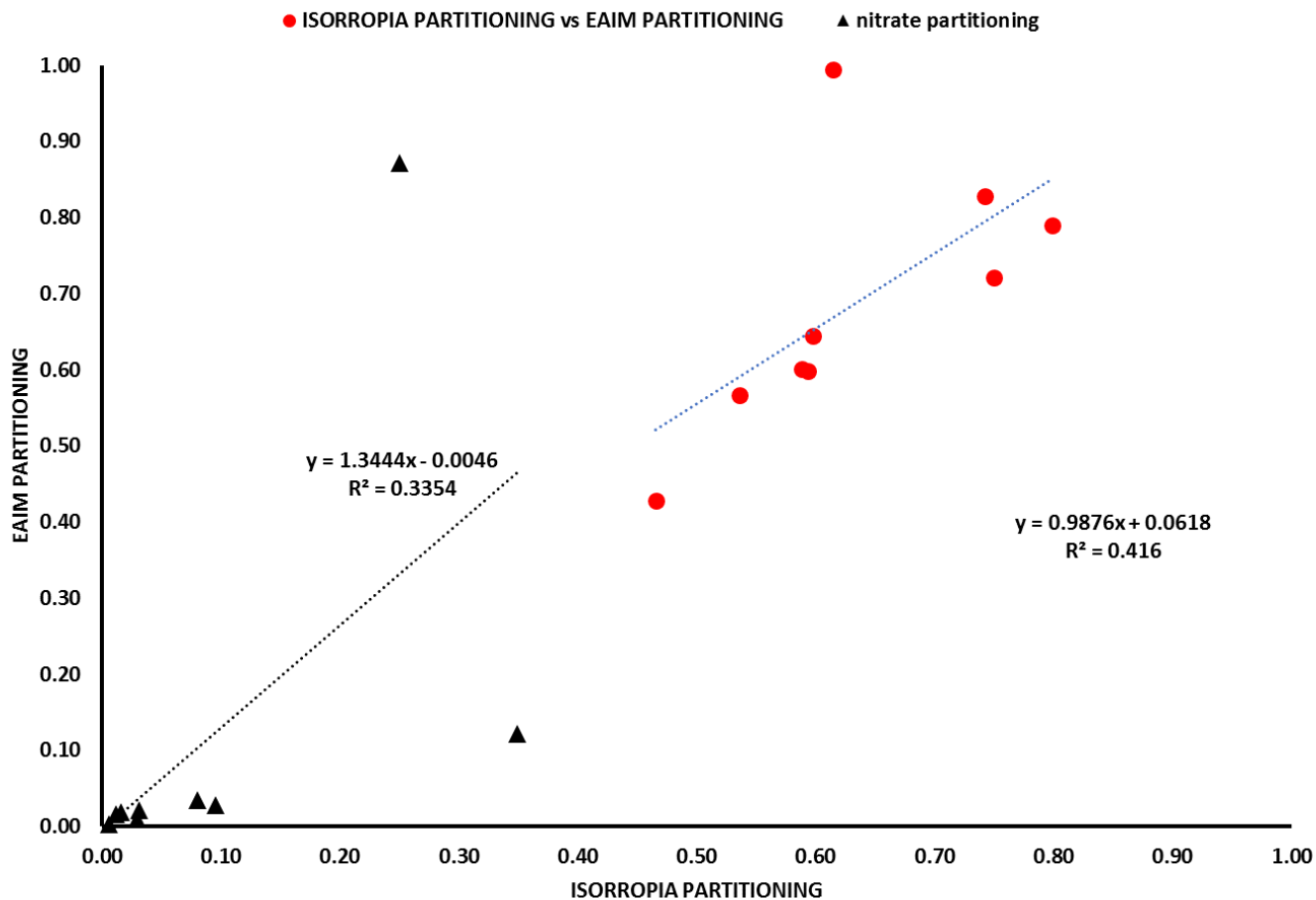
55 When comparing the total aerosol partitioning (particle to gas) for each SEARCH site  
56 between ISORROPIA and E-AIM, they compare favorably, displaying an almost linear correlation  
57 between the two (Fig. S7). For the low temperatures of December in Yorkville ( $\bar{T} \leq 10^{\circ}\text{C}$ ) E-AIM  
58 predicts a near complete absence of gas phase, in contrast to ISORROPIA, which is attributed to  
59 the difference of how the activity coefficients are calculated between the two models (Wexler &  
60 Clegg 2002, Friese & Ebel 2010, Clegg et al. 1992). Acidity between the two models differs, but  
61 both predict sufficiently low values for pH for all sites (Table S2).

62 Initially, an amount of 25 or 50% of additional oxalic acid on a mole basis was added to  
63 the baseline case, and then the pH was compared (Table S2). We find that for the cases presented  
64 in this study, addition of organic compounds to the model did not have a significant impact on  
65 acidity when compared to the baseline run, apart from the cases where RH was higher than 80%  
66 and the mole fraction of organic acids in the aqueous phase is greater than 25%. pH remains rather  
67 insensitive to the addition of oxalic acid for most cases, apart from the case that has the highest  
68 RH=0.8, and subsequently the highest amount of liquid water. For all other cases, most of oxalic  
69 acid partitions to the gas phase and its impact is negligible. Similarly, when other organic acids  
70 are tested against the baseline, under the same conditions (maleic, succinic, malonic), they incur  
71 a maximum 4% change on pH (Table S3).

72 For the substitution tests with oxalic acid, removal of sulfate from the system rapidly  
73 decreases the amount of total water in the particulate phase (Fig. S8). This leads to the partitioning  
74 of organics to the gas phase (Fig. S8), abating their impact on pH, since the relative composition  
75 on a mole fraction basis remains largely the same.

76 The above analysis demonstrates that, for the cases presented in this paper, organics do not  
77 have an appreciable impact on pH when only one liquid phase exists. Allowing more than one  
78 liquid phase of different compositions to form, can still potentially impact pH (Pye et al. 2018).





79

80

81 **Figure S7** –Nitrate (black) and total (red) particle-to-gas partitioning predicted between E-AIM  
 82 and ISORROPIA.

83

84

85

86

87

88

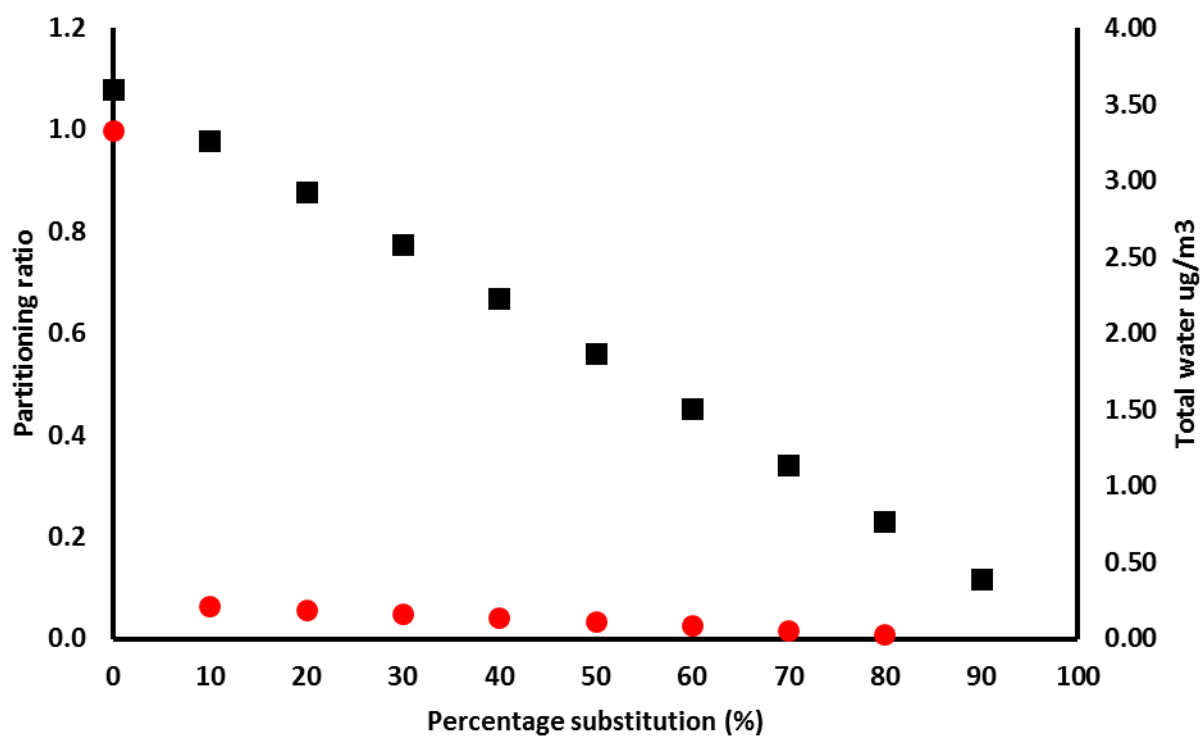
89

90

91 **Table S2** – ISORROPIA, E-AIM and E-AIM with an additional 25 and 50% oxalic acid  
 92 predicted pH for all sites.

ISORROPIA PH	pH EAIM	pH 25% OXALIC	pH 50% OXALIC
-0.22	0.81	0.82	0.83
-0.30	0.92	0.92	0.91
0.55	1.31	1.32	1.25
-0.04	0.91	0.90	0.83
-0.01	0.55	0.55	0.55
0.07	0.34	0.34	0.34
0.14	0.53	0.53	0.52
-0.46	0.91	0.71	0.57
1.49	1.00	1.10	1.18

93  
 94



95  
 96 **Figure S8** –Comparison of predicted particle-to-gas partitioning of oxalic acid (red)  
 97 water (black) between E-AIM and ISORROPIA as a function of sulfate substitution to oxalic  
 98 acid.

99

100 **Table S3** – E-AIM predicted pH for the baseline case and for the cases with 25 and 50%  
 101 addition of maleic, succinic or malonic acid.

<b>Default pH EAIM</b>	
0.809500489	
<b>pH 25% MALEIC</b>	<b>pH 50% MALEIC</b>
0.827689031	0.832387327
<b>pH 25% SUCCINIC</b>	<b>pH 50% SUCCINIC</b>
0.821886748	0.821886748
<b>pH 25% MALONIC</b>	<b>pH 50% MALONIC</b>
0.81276138	0.808548986

102

103

104 **The role of non-volatile cations in PM 2.5 pH**

105 To test whether the PM 2.5 pH bias can be attributed to the internally-mixed NVCs, we  
 106 omit their presence and repeat the aerosol thermodynamic calculations (offline) for 2001 and 2011.  
 107 The pH values of 2011 plotted against 2001 for each grid cell in the Eastern US study domain, for  
 108 the winter (a) and summer (b) seasons are shown in Figure S10. On a seasonal basis, when NVCs  
 109 are included in the thermodynamic calculations, for the winter the strongest biases are observed  
 110 for gridcells that in 2001 had pH between -1 and 3, with differences becoming smaller with  
 111 increasing pH. The largest differences during summer are localized for the gridcells that had pH  
 112 values between -1 and 0.5 in 2001, while some gridcells from the Southern Lake Michigan and  
 113 the coastal area of Massachusetts, New Hampshire, Maine and South Carolina exhibit very strong  
 114 biases of 5 to 3 units. The proximity to marine aerosol and non-volatile Na is the underlying reason  
 115 for this large change in aerosol pH.

116 With the removal of these NVCs and sea salt, there is remarkable agreement between the  
 117 2001 and 2011 predicted PM<sub>2.5</sub> pH, with only a small positive bias for the grid cells that in 2001  
 118 had a pH of less than unity (Fig. S9). Although NVCs can sometimes comprise a significant

119 portion of PM<sub>2.5</sub>, as it was the case for the SOAS campaign (Allen et al. 2015, Bondy et al. 2017),  
 120 on average they should not be a major constituent of PM<sub>2.5</sub> (Guo et al. 2015) over the Eastern  
 121 US, which is indicative of a portion of coarse mode dust being distributed to the smaller sized  
 122 aerosol in CMAQ, contrary to what has thus far been observed (Foroutan et al. 2017). While the  
 123 dust emissions were the same between the 2001 and 2011 simulations, given the same meteorology  
 124 for these years, and the fact that they were not scaled up/down in our model emissions, their impact  
 125 became much larger in 2011 due to the reductions in sulfate. NVCs on average account for 0.39  
 126  $\mu\text{g m}^{-3}$  of CMAQ PM<sub>2.5</sub> both in 2011 and 2001 over the Eastern US, which a factor of 4 higher  
 127 than the measured PM<sub>1</sub> NVCs during the WINTER campaign (Guo et al. 2016). There is no bias  
 128 for the gridcells near coastal areas for this case, indicating that these areas were strongly affected  
 129 by the abundance of sea salt aerosol in fine PM.

130 To verify this finding, we compared observations of NVCs from the Metrohm Monitor for  
 131 AeRosol and Gases (MARGA) for the SOAS campaign, as well as the SEARCH and CSN sites,  
 132 to CMAQ results. The average mass of modelled NVCs for these sites is 0.56  $\mu\text{g m}^{-3}$ , when  
 133 compared to 0.14  $\mu\text{g m}^{-3}$  for the SEARCH/CSN average, indicating a factor of 4 overestimation,  
 134 mainly from crustal elements ( $\text{K}^+$ ,  $\text{Ca}^{+2}$  and  $\text{Mg}^{+2}$ ), further corroborated by the findings of Pye et  
 135 al. 2018, where the same comparison was carried out.

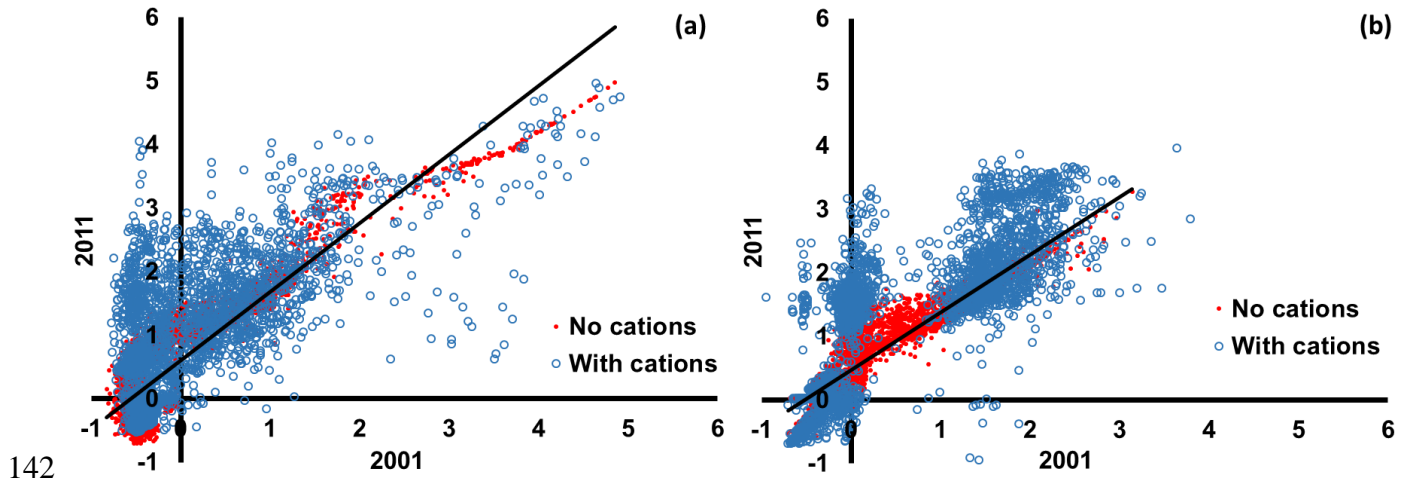
136  
 137

138 **Table S4** – Comparison of NVCs ( $\mu\text{g m}^{-3}$ ) between simulation results for the 3 SEARCH  
 139 sites, and the measurements provided in Allen et al. 2015 and Pye et al. 2018

140

	Na	Mg	K	Ca	Total NVCs
<b>JST AUG</b>	0.024	0.033	0.135	0.462	<b>0.653</b>
<b>JST MAY</b>	0.039	0.040	0.146	0.473	<b>0.697</b>
<b>JST NOV</b>	0.053	0.049	0.192	0.533	<b>0.826</b>
<b>JST SEP</b>	0.029	0.038	0.155	0.450	<b>0.671</b>
<b>YRK DEC</b>	0.052	0.044	0.184	0.412	<b>0.692</b>
<b>YRK JUL</b>	0.014	0.010	0.063	0.098	<b>0.185</b>
<b>CSN</b>	0.050	0.000	0.060	0.030	<b>0.140</b>
<b>SEARCH</b>	0.050	-	0.060	0.030	<b>0.140</b>
<b>SOAS</b>	0.032	0.007	0.071	0.083	<b>0.193</b>
<b>MARGA</b>	0.074	0.010	0.045	0.047	<b>0.175</b>

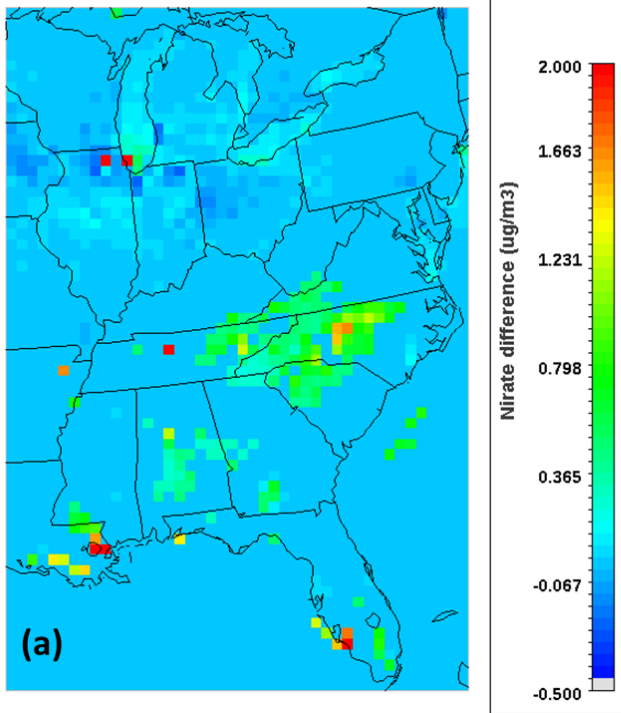
141



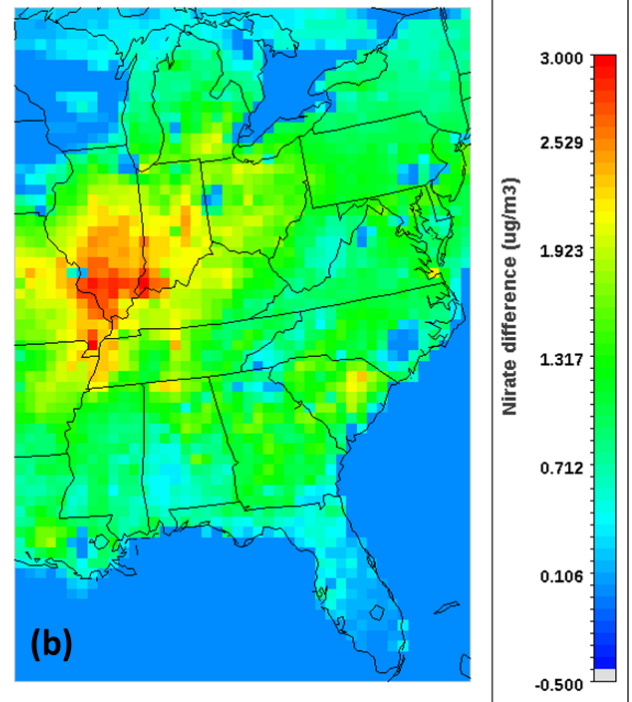
142

143 **Figure S9** - Scatter plots of ISORROPIA predicted pH over the Eastern US study domain, for the  
 144 winter (a) and summer (b), with and without NVCs.

**Nitrate difference for July 2011**



**Nitrate difference for January 2011**

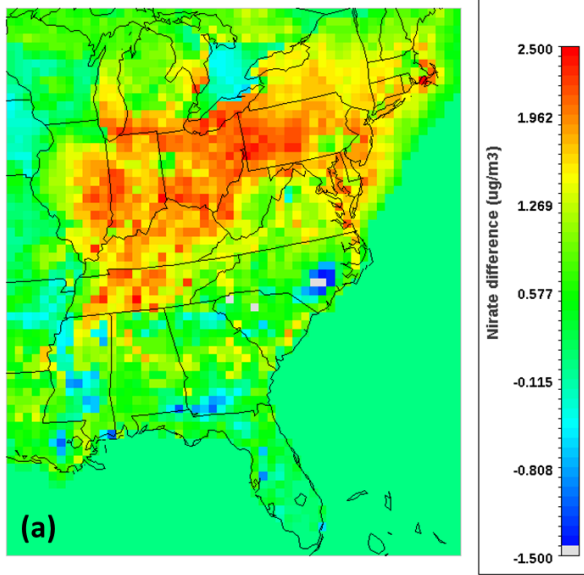


145

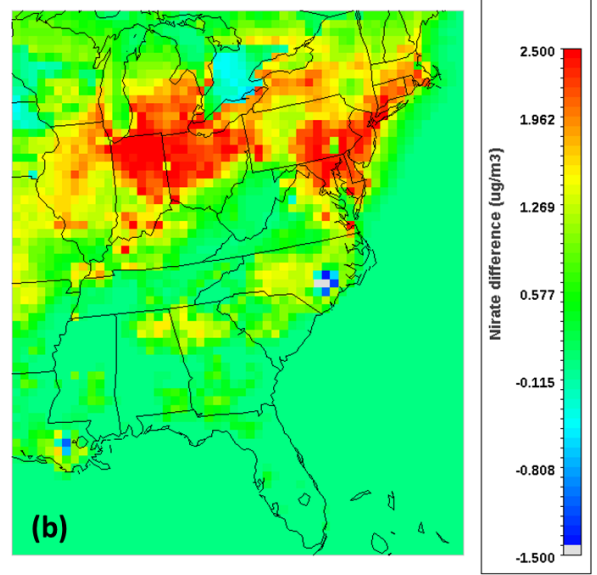
146 **Figure S10** – Difference in nitrate over the Eastern US, between ISORROPIA predicted nitrate  
 147 when NVCs are included in calculations, and when they are excluded, for July (a) and January (b)  
 148 of 2011.

149

Difference of 2011 to 2001 NO3 with NVCs included



Difference of 2011 to 2001 NO3 without NVCs



150

151 **Figure S11** – Difference in predicted nitrate over the Eastern US between 2011 and 2001 when  
152 NVCs are included in calculations (a), and when they are excluded (b).

153

154

155 **References**

- 156 Allen, H. M., D. C. Draper, B. R. Ayres, A. Ault, A. Bondy, S. Takahama, R. L. Modini, K.  
157 Baumann, E. Edgerton, C. Knote, A. Laskin, B. Wang, and J. L. Fry (2015), Influence of crustal  
158 dust and sea spray supermicron particle concentrations and acidity on inorganic NO<sub>3</sub><sup>-</sup> aerosol  
159 during the 2013 Southern Oxidant and Aerosol Study, *Atmospheric Chemistry and Physics*,  
160 15(18), 10669-10685.
- 161 Bondy, A. L., B. Wang, A. Laskin, R. L. Craig, M. V. Nhliziyo, S. Bertman, K. A. Pratt, P. B.  
162 Shepson, and A. P. Ault (2017), Inland Sea Spray Aerosol Transport and Incomplete Chloride  
163 Depletion: Varying Degrees of Reactive Processing Observed during SOAS, *Environmental*  
164 *Science & Technology*.
- 165 Clegg, S. L., Pitzer, K. S., and Brimblecombe, P., Thermodynamics of multicomponent, miscible,  
166 ionic solutions. II. Mixtures including unsymmetrical electrolytes. *J. Phys. Chem.* 96, 9470-9479,  
167 DOI: 10.1021/j100202a074, 1992
- 168 Foroutan, H., J. Young, S. Napelenok, L. Ran, K. W. Appel, R. C. Gilliam, and J. E. Pleim (2017),  
169 Development and evaluation of a physics-based windblown dust emission scheme implemented  
170 in the CMAQ modeling system, *J. Adv. Model. Earth Syst.*, 9, 585–608,  
171 doi:10.1002/2016MS000823.
- 172 Friese, E. and Ebel, A., Temperature dependent thermodynamic model of the system H<sup>+</sup> - NH<sub>4</sub><sup>+</sup>  
173 - Na<sup>+</sup> - SO<sub>4</sub><sup>2-</sup> - NO<sub>3</sub><sup>-</sup> - Cl<sup>-</sup> - H<sub>2</sub>O. *J. Phys. Chem. A*, 114, 11595-11631, DOI:  
174 10.1021/jp101041j, 2010
- 175 Guo, H., Sullivan, A.P., Campuzano-Jost, P., Schroder, J.C., Lopez-Hilfiger, F.D., Dibb, J.E.,  
176 Jimenez, J.L., Thornton, J.A, Brown, S.S., Nenes, A., and Weber, R.J. (2016) Fine particle pH and  
177 the partitioning of nitric acid during winter in the northeastern United States, *J.Geoph.Res.*, 121,  
178 doi:10.1002/2016JD025311
- 179 Guo, H., Xu, L., Bougiatioti, A., Cerully, K. M., Capps, S. L., Hite Jr., J. R., Carlton, A. G., Lee,  
180 S.-H., Bergin, M. H., Ng, N. L., Nenes, A., and Weber, R. J.: Fine-particle water and pH in the



181 southeastern United States, *Atmos. Chem. Phys.*, 15, 5211-5228, doi:10.5194/acp-15-5211-2015,  
182 2015.

183 Pye, H. O. T., Zuend, A., Fry, J. L., Isaacman-VanWertz, G., Capps, S. L., Appel, K. W., Foroutan,  
184 H., Xu, L., Ng, N. L., and Goldstein, A. H.: Coupling of organic and inorganic aerosol systems  
185 and the effect on gas–particle partitioning in the southeastern US, *Atmos. Chem. Phys.*, 18, 357-  
186 370, <https://doi.org/10.5194/acp-18-357-2018>, 2018.

187 Wexler, A. S., and S. L. Clegg, Atmospheric aerosol models for systems including the ions H<sup>+</sup>,  
188 NH<sub>4</sub><sup>+</sup>, Na<sup>+</sup>, SO<sub>4</sub><sup>2-</sup>, NO<sub>3</sub><sup>-</sup>, Cl<sup>-</sup>, Br<sup>-</sup>, and H<sub>2</sub>O, *J. Geophys. Res.*, 107(D14), DOI:  
189 10.1029/2001JD000451, 2002, <http://www.aim.env.uea.ac.uk/aim/aim.php>

190

191